ACS APPLIED MATERIALS & INTERFACES

Research Article

www.acsami.org

Graphene Oxide Based Nanocarrier Combined with a pH-Sensitive Tracer: A Vehicle for Concurrent pH Sensing and pH-Responsive Oligonucleotide Delivery

Chia-Jung Hsieh,[†] Yu-Cheng Chen,[†] Pei-Ying Hsieh,[‡] Shi-Rong Liu,[†] Shu-Pao Wu,[†] You-Zung Hsieh,[†] and Hsin-Yun Hsu*[,†,‡,§]

[†]Department of Applied Chemistry, [‡]Center for Interdisciplinary Science (CIS), and [§]Institute of Molecular Science, National Chiao-Tung University, No. 1001 Ta-Hsueh Road, Hsinchu 30010, Taiwan

Supporting Information

ABSTRACT: We chemically tuned the oxidation status of graphene oxide (GO) and constructed a GO-based nanoplatform combined with a pH-sensitive fluorescence tracer that is designed for both pH sensing and pH-responsive drug delivery. A series of GOs oxidized to distinct degrees were examined to optimize the adsorption of the model drug, poly dT_{30}. We determined that highly oxidized GO was a superior drug-carrier candidate in vitro when compared to GOs oxidized to lesser degrees. In the cell experiment, the synthesized pH-sensitive rhodamine dye was first applied to monitor cellular pH; under acidic conditions, protonated rhodamine fluoresces at 588 nm (λ_{ex} = 561 nm). When the dT_{30}-GO nanocarrier was introduced into cells, a rhodamine-triggered competition reaction occurred, and this led to the release of the oligonucleotides and the quenching of rhodamine fluorescence by GO. Our results indicate high drug loading (FAM-dT_{30}/GO = 25/50 μg/mL) and rapid cellular uptake (<0.5 h) of the nanocarrier which can potentially be used for targeted RNAi delivery to the acidic milieu of tumors.

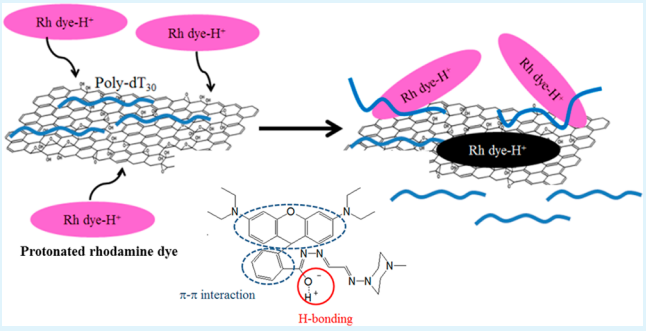

KEYWORDS: *graphene oxide, pH-responsive drug delivery, pH-sensitive rhodamine, oligonucleotide delivery, theranostics*

INTRODUCTION

The advent of nanotechnology has led to the development of a new dimension in cancer treatment, theranostics, in which diagnostics and therapeutics are combined in order to improve health-care management in clinics. In this research area, the development of molecular diagnostic tools and targeted therapeutics is interconnected, with the aim being to enable smart drug release. In cancer chemotherapy, small-molecule anticancer drugs such as doxorubicin (DOX) or camptothecin (CPT) have been widely used. However, the poor water solubility of these drugs and the severe systemic side effects caused by their nonspecific targeting of healthy tissues are major problems that must be tackled. Conversely, gene therapy has emerged as a new strategy for treating genetic diseases such as cystic fibrosis, Parkinson's disease, and cancer,[1] but two challenges must be overcome in this case: (1) oligonucleotides must be protected from nuclease degradation and (2) cellular oligonucleotide-uptake efficiency must be enhanced.[2]

Recently, graphene oxide (GO), a carbon nanomaterial featuring a 2-D structure, covalently or noncovalently functionalized with small molecular drugs, DNA/RNA, antibodies, proteins, or genes has been employed in numerous applications such as drug delivery,[3] biological detection,[4,5] bioimaging,[5] and sensing.[6] GO holds considerable potential for meeting the therapy requirements mentioned previously,[3,5] and because of its ultrahigh surface area, GO can be loaded with larger amounts of drugs than can other carbon materials. The π-conjugated GO enables versatile opsonization, and hydrophobic anticancer drugs can be readily adsorbed on the surface of GO in order to facilitate the cellular uptake of the particulates. Previous studies have reported that GO can protect nucleotides from degradation.[7,8] Feng et al.[9] and Zhang et al.[10] used the cationic polymer polyethylenimine (PEI) to functionalize GO, and the PEI-GO nanocomposite was used for introducing plasmid DNA (pDNA) into HeLa cells. Feng et al.[9] compared the transfection efficiency of PEI-GO-pDNA with that of the conventional PEI-pDNA carrier that does not include GO. Grafting on GO substantially lowered the cytotoxicity of PEI, and the transfection efficiency was enhanced as a result of the proton-sponge effect that triggers the endosomal release of pDNA. This design was further developed by Kim and Kim,[11] who used near-infrared (near-IR) light (808 nm, 6 W/cm^2) to irradiate a complex—PEGylated branched-PEI-conjugated reduced-GO harboring pDNA (PEG-

Received: March 18, 2015
Accepted: May 6, 2015
Published: May 6, 2015

DOI: 10.1021/acsami.5b02397
ACS Appl. Mater. Interfaces 2015, 7, 11467−11475

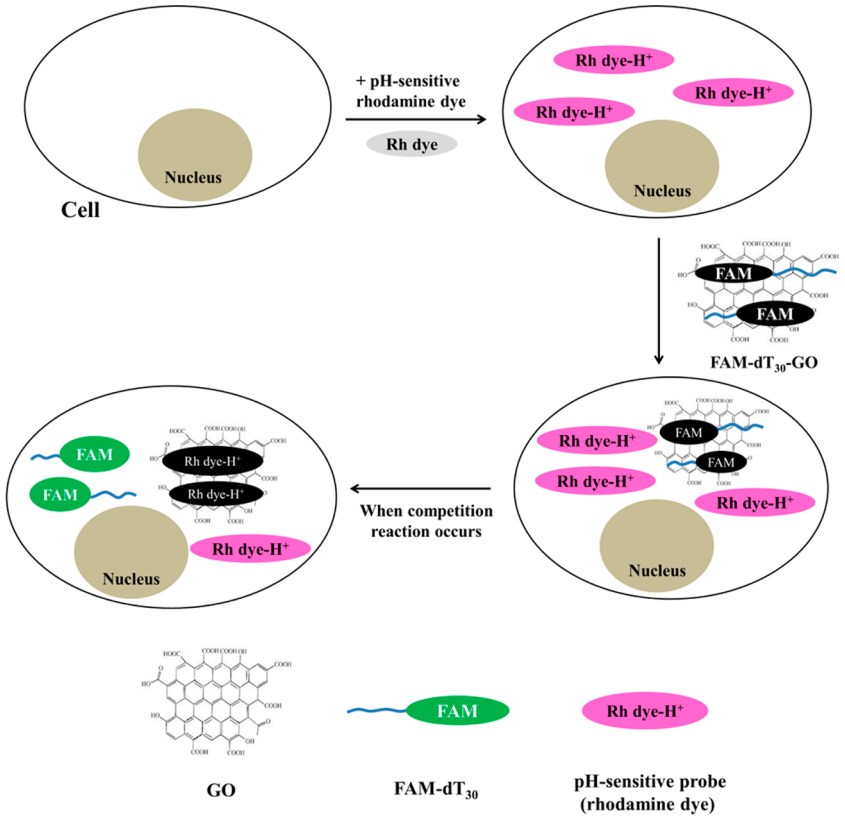

Figure 1. Proposed mechanism of GO-based simultaneous pH sensing and oligonucleotide delivery.

BPEI-rGO/pDNA)—and demonstrated that after introducing this complex into PC3 and NIH/3T3 cells, increasing the temperature induced the rupture of the endosomal membrane and the release of the pDNA.

In addition to using external stimuli to trigger the delivery of therapeutics, researchers have designed novel nanoplatforms for enabling the sensing of internal stimuli in cells or tissue environments, thereby making it possible to obtain a response suitable for the transport and delivery of materials to a given location at a specific time. One of these approaches involves eliciting a response to internal pH, which varies substantially in disease states such as ischemia, infection, inflammation, and cancer. Because the metabolism (rate of glycolysis) is highly active in tumor cells under both aerobic and anaerobic conditions, the tumor microenvironment is highly acidic when compared to that of normal tissues.[12−15] Consequently, exploiting the acidic pH of the cancer environment has proven to be a powerful and effective strategy for designing a new generation drug-delivery systems. In the case of drug release in acidic environments, hydrophobic drugs such as DOX,[3,5,16] CPT,[3,17] or 5-fluorouracil (5-FU)[18,19] can be protonated under low-pH conditions, and this weakens the $\pi-\pi$ and hydrophobic interaction and the hydrogen bonding between the drug and GO and leads to drug release. Other nonaromatic drugs such as metformin hydrochloride (MFH), an antidiabetic drug, can form supramolecular hydrogels with GO through supramolecular assembly. MFH was released from GO in a highly acidic environment (pH = 1) because both GO and MFH were almost completely protonated, and this disrupted the hydrogen bonds and the electrostatic attraction between GO and MFH.[20]

Based on the reviewed literature on GO-based, pH-controlled drug release, and to the best of our knowledge, most studies to date have focused on the delivery of small molecular drugs rather than on gene delivery, although GO-based biosensors have been increasingly developed for oligonucleotide,[21−24] small drug,[25] and cell[26] analysis. We proposed that GO could serve not only as a sensing nanodevice but also as a great carrier for oligonucleotide-based drugs. The oligonucleotides have several unique advantages over conventional small molecular drugs as they are inherently nontoxic and highly specific to their targets; we designed a new gene-delivery system, in which GO was chemically tuned at different oxidation status to enable simple and stable adsorption of oligonucleotides without necessity to employ additional cationic polymers during fabrication. This GO-based platform combined with a novel pH-sensitive rhodamine fluorescence probe was used for concurrent pH sensing and the corresponding drug release monitoring.

The nanocarrier design that we used was inspired by the study of Chen and Zhang,[27] who investigated the competitive binding reaction of various polyaromatic fluorescent molecules in order to enable the release of single-stranded DNA (ssDNA) from single-walled carbon nanotubes (SWNTs). Chen and Zhang proposed that positively charged small molecules might readily approach the negatively charged ssDNA-SWNTs and thereby allow the extended aromatic rings of the dye molecules to compete with ssDNA for binding SWNTs through $\pi-\pi$ interaction. Based on the proposed mechanism and the widely recognized fluorescence-quenching effect of GO, we used a novel pH-sensitive rhodamine together with the GO nanocarrier in order to enable the monitoring of intracellular gene delivery in an acidic milieu (Figure 1). As a model drug, we used poly dT_{30}. Once protonated under low-pH conditions, the pH-sensitive rhodamine fluoresces and also competes with the

DOI: 10.1021/acsami.5b02397
ACS Appl. Mater. Interfaces 2015, 7, 11467−11475

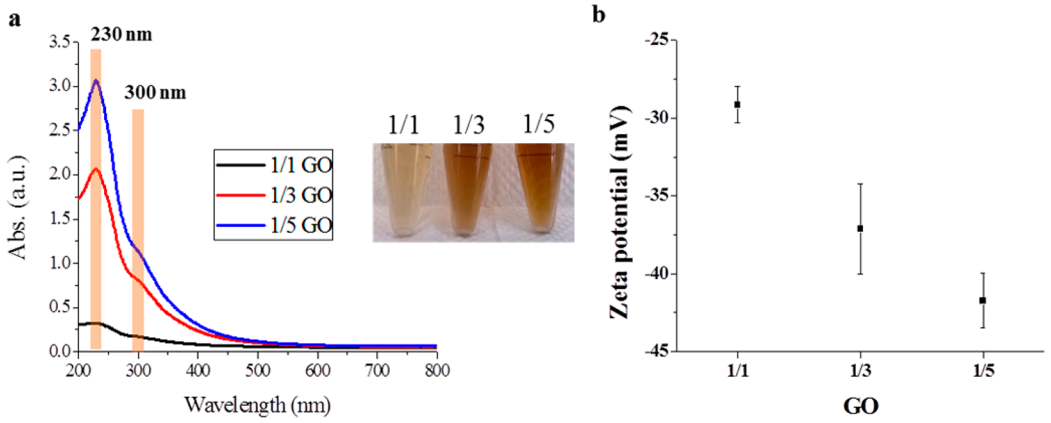

Figure 2. (a) UV−vis spectra and (b) ζ potentials of GOs at different oxidation status (an increase in the oxidation degree from 1/1 GO to 1/5 GO).

poly dT_{30} adsorbed on the GO surface. The binding of rhodamine on GO leads to the quenching of its fluorescence and promotes the release of the oligonucleotides. We further validated this proposed mechanism by using 6-carboxyfluorescein (FAM)-labeled-poly dT_{30} (FAM-dT_{30}): the turning-on of FAM fluorescence allowed us to monitor the release of the oligonucleotides from the GO nanocarrier.

EXPERIMENTAL SECTION

Chemicals. The following reagents and materials were from commercial sources: expandable graphite (Homytech Auto Parts Co. Ltd., Bade City, Taiwan); potassium permanganate ($KMnO_4$) (J. T. Baker, Center Valley, PA, USA); 95%−97% sulfuric acid (H_2SO_4), hydrochloric acid (HCl), and 30% (w/w) hydrogen peroxide (H_2O_2) (Sigma-Aldrich, St. Louis, MO, USA); ssDNA (dA_{12}, dT_{12}; Mission Biotech Co. Ltd., Taipei, Taiwan); FAM-dT_{30} and SYBR Gold (MDBio, Inc., Taipei, Taiwan); cell mask deep red plasma membrane stain (Life Technologies Co. Ltd., Taipei, Taiwan); Nanosep centrifugal devices fit with Omega membrane MWCO 100 kDa filters (Pall Corp., Port Washington, NY, USA); tris-acetate-EDTA (TAE) buffer (UniRegion Bio-Tech Co. Ltd., Hsinchu, Taiwan); agarose and 2.5 mM dNTPs (Focus Biotech Sdn. Bhd., Petaling Jaya, Malaysia); and DNA polymerase and PCR buffer (Bersing Tech. Co. Ltd., Hsinchu, Taiwan). The pH-sensitive rhodamine dye was derived by modifying rhodamine B hydrazine with 2- (*N*-methylpiperazinylimino) acetaldehyde (Supporting Information Figure S1)[28] and was kindly provided by Prof. Shu-Pao Wu (National Chiao-Tung University, Hsinchu, Taiwan). The cell line raw 264.7 was obtained from Food Industry Research and Development Institute (Hsinchu, Taiwan). Dulbecco's modified eagle's medium (DMEM) and fetal bovine serum (FBS) were purchased from Life Technologies, and Trypsin-EDTA was from Biowest Co. Ltd., Nuaillé, France. Sterilized deionized (DI) water was used throughout the work.

Synthesis of GO Oxidized to Distinct Degrees. GO was prepared according to the modified Hummers' method.[29] GOs were oxidized to distinct degrees by changing the mass ratio of graphite and $KMnO_4$, and these GOs were denoted as 1/1, 1/3, and 1/5 GOs. Briefly, expandable graphite (0.5 g) was mixed with 95−97% H_2SO_4 (12.5 mL) in an ice bath, and then $KMnO_4$ (0.5, 1.5, or 2.5 g) was gradually added to this solution. While adding $KMnO_4$, the temperature must be maintained below 20 °C. After $KMnO_4$ was added, the mixture was stirred at 45 °C for 2 h. During this process, the mixture turned from green to brown and became too dense to allow easy stirring. The mixture was diluted with 23 mL of DI water, which increased the temperature to 95 °C, and after stirring the diluted mixture vigorously for 15 min at 95 °C, 70 mL of DI water and 5 mL of H_2O_2 were added to it. The color now changed from brown to yellow, and this indicated the successful synthesis of GO. The resulting GO solution was washed three times with 5% (v/v) HCl and then five times with DI water by using centrifugation and then was lyophilized to obtain the purified powder.

Synthesis of Oligonucleotide-Immobilized GO. We mixed 200 μg/mL solutions of GO oxidized to distinct degrees (1/1, 1/3, and 1/5) with 100 μg/mL oligonucleotide dT_{30} (v/v = 1/1) and sonicated the mixture for 30 min. The free dT_{30} was removed using a 100-kDa-cutoff filter, and the precipitates were recovered using DI water.

Characterization of the GO Nanocomposite. Fourier transform infrared (FT-IR) spectra were measured using an FT/IR-6100 spectrometer (JASCO International Co., Ltd., Tokyo, Japan), and UV−vis spectra were recorded using a Multiskan GO microplate spectrophotometer (Thermo Fisher Scientific Inc. Waltham, MA, USA). ζ potentials were measured using a Delsa Nano C particle analyzer (Beckman Coulter Inc., Brea, CA, USA). Transmission electron microscopy (TEM) images (Supporting Information Figure S2) were obtained using the microscope JEM-ARM200FTH (JEOL Ltd., Tokyo, Japan). Energy-dispersive X-ray spectroscopy (EDS) analysis (Supporting Information Figure S3) was performed using an Oxford INCA Energy 350 system (Oxford Instruments plc, Oxfordshire, U.K.). Dynamic light scattering (DLS) results (Supporting Information Figure S4) were obtained using a Particle Size Analyzer 90 Plus (Brookhaven Instruments Corp., Holtsville, NY, USA).

Competition Reaction in Vitro. Competitive and noncompetitive reactions were performed by mixing purified dT_{30}-GO ([GO], 100 μg/mL; [dT_{30}], 50 μg/mL) with or without rhodamine (100 μM) in PBS of various pH (4−7), respectively, and incubating the mixture overnight in the dark at room temperature (RT). The supernatant was then recovered after centrifugation (12,000 rpm, 10 min) and analyzed by performing polymerase chain reaction (PCR). The supernatant was mixed with DNA primers (1 mg/mL dA_{12} and dT_{12}), 10× PCR buffer (100 mM Tris-HCl, pH 8.3 at 25 °C; 500 mM KCl; 15 mM $MgCl_2$; 0.01% gelatin), dNTP mixture (2.5 mM), DNA polymerase (250 U), and DI water, and the oligonucleotide was amplified in a PCR machine (Labcycler, SensoQuest). Lastly, the products were analyzed by means of agarose (4%) electrophoresis and imaged using an Image Quant LAS 4000 system (GE Healthcare Life Sciences).

Oligonucleotide Delivery into Raw 264.7 Cells through Competition Reaction. Raw 264.7 cells were routinely cultured in DMEM supplemented with 10% FBS at 37 °C in a humidified atmosphere containing 5% CO_2. The uptake of rhodamine (λ_{ex} = 561 nm; λ_{em} = 588 nm) by raw 264.7 cells was evaluated by incubating the cells in 8-well plates (4×10^4 cells/well) in the presence of rhodamine at a final concentration of 100 μM for 0.5, 1, or 2 h in order to optimize the time required for dye uptake. Oligonucleotide delivery by the GO nanocomposite was examined using FAM-dT_{30}-1/5 GO ([1/5 GO], 50 μg/mL; [FAM-dT_{30}], 25 μg/mL); delivery was monitored at various incubation times (0.5, 1, and 2 h) after 0.5 h of rhodamine uptake and washing to remove free dye molecules. For imaging, cells

DOI: 10.1021/acsami.5b02397
ACS Appl. Mater. Interfaces 2015, 7, 11467−11475

were washed two times with PBS, and then their nuclei were stained with Hoechst 33342, after which the cells were examined using a confocal laser scanning microscope (Leica TCS SP5, Leica Microsystems Inc., Buffalo Grove, IL, USA).

Flow cytometric analysis was performed by incubating raw 264.7 cells in 24-well plates (3×10^5 cells/well) and then using exactly the same experimental procedures as those used for preparing cells for confocal imaging. Briefly, after 0.5 h of rhodamine uptake and washing to remove free dye molecules, FAM-dT_{30}-1/5 GO (final concentration of GO = 50 μg/mL, with 25 μg/mL immobilized FAM-dT_{30}) was added and the cells were incubated for various times (0.5, 1, and 2 h). The cells were then washed two times with PBS and analyzed using the flow cytometric platform MoFlo XDP (Beckman Coulter, Indianapolis, IN, USA).

Safety Considerations. ***Caution!*** *Preparation of oxidized GO required the use of dehydrating agents sulfuric acid and oxidants including $KMnO_4$ and H_2O_2, which should be handled with extreme care in fume cupboards. Skin or eye contact and accidental inhalation or ingestion should be avoided.*

RESULTS AND DISCUSSION

GOs oxidized to various degrees were prepared using a modified Hummer's method[29] and characterized based on their UV−vis spectra (Figure 2a) and ζ potentials (Figure 2b). A main absorption peak at 230 nm and a shoulder peak at 300 nm were observed in all three types of oxidized GO. Table 1 lists

Table 1. Absorbance Coefficients at 230 nm of GOs Oxidized to Distinct Degrees (Oxidation Degree Increased from 1/1 GO to 1/5 GO)

types of GO	1/1 GO	1/3 GO	1/5 GO
ε (L g^{-1} cm^{-1})	30.98	36.44	44.60

the extinction coefficients at 230 nm of GOs oxidized to distinct degrees and shows that the value increased with increasing degree of oxidation. As expected, the oxidized GOs were negatively charged because oxygenated groups such as hydroxyl and carboxylic groups, which are electronegative, could be generated during oxidation (Figure 2b). With an increase in the oxidation degree (from 1/1 GO to 1/5 GO), the amounts of electronegative groups also increase, and thus the negative charge on GO is enhanced. This conclusion was supported by the FT-IR spectra obtained (Figure 3a), which revealed enhanced absorption at the wavenumbers of the oxygenated functional groups C−O (1050 cm^{-1}), C−O−C (1250 cm^{-1}), C−OH (1400 cm^{-1}), and aldehyde C−H (2800−3000 cm^{-1}) in the highly oxidized GO (1/5) comparing with graphite and GOs at other oxidation status (Figure 3b).

Next, the nanocomposite dT_{30}-GO was synthesized by means of simple physical adsorption of poly dT_{30} through $\pi-\pi$ stacking with GO. The UV−vis spectra of 1/5 GO, poly dT_{30}, and the dT_{30}-1/5 GO nanocomposite are shown in Figure 4 (similar characteristic peaks were also found in 1/1 and 1/3 GO; for easy visualization only 1/5 GO was shown here). The peaks at 210 and 260 nm are derived from dT_{30}, whereas the peak at 300 nm is from GO. The spectra indicated successful synthesis of the dT_{30}-GO nanocomposite.

Before delivering the GO-based nanocarrier into cells, we examined the competitive reaction between rhodamine and dT_{30}-GO under various pH conditions in vitro. We synthesized GOs oxidized to distinct degrees and investigated the adsorption of poly dT_{30} on these GOs. At each specified pH, we performed the competitive reaction together with a noncompetitive control. The dT_{30}-GO solution was incubated

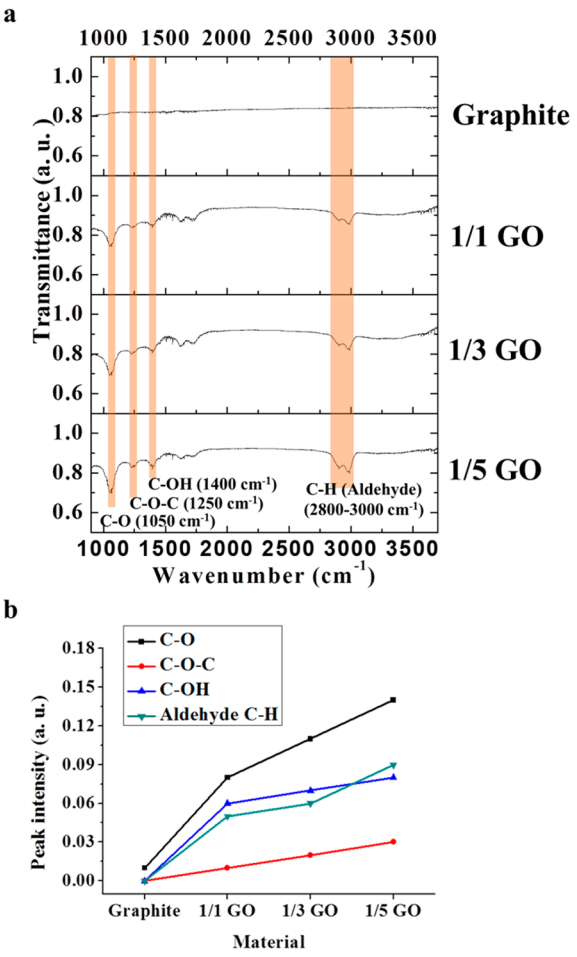

Figure 3. (a) FT-IR spectra of graphite and GOs at different oxidation status (an increase in the oxidation degree from 1/1 GO to 1/5 GO). (b) The IR peak intensity was calculated according to the spectra in panel a at each identified functional groups.

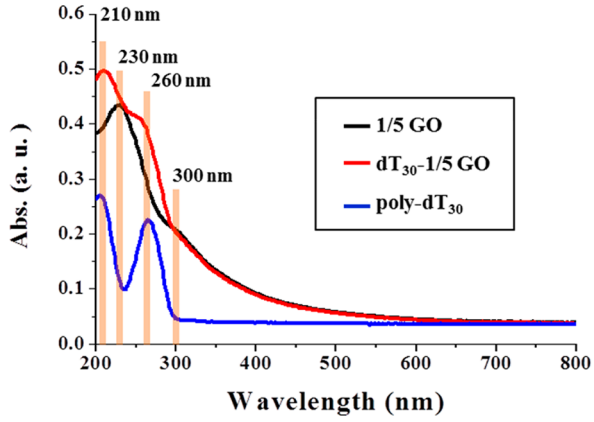

Figure 4. UV−vis spectra of poly dT_{30}, 1/5 GO, and dT_{30}−1/5 GO.

with and without rhodamine (dissolved in PBS of specified pH) in the competitive and noncompetitive experiments, respectively. We used PBS of various pH values to mimic the cellular milieu. The reactions were performed in the dark overnight, and then high speed centrifugation was used to precipitate the dT_{30}-GO. The collected supernatants were used for examining the amounts of dT_{30} released in the two test groups. The released poly dT_{30} was quantified using PCR followed by

DOI: 10.1021/acsami.5b02397
ACS Appl. Mater. Interfaces 2015, 7, 11467−11475

agarose gel electrophoresis (Figure 5). A comparison of the three agarose gels shows that poly dT_{30} was readily released

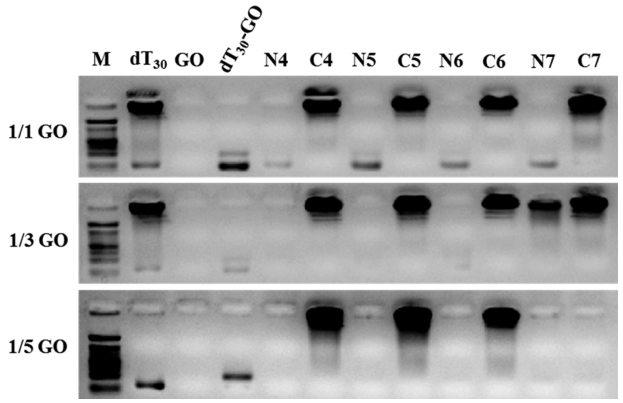

Figure 5. Agarose gel electrophoresis results of the competition reaction (competition group (C) and noncompetition group (N) were dT_{30}-GO incubated with or without pH-sensitive rhodamine dye in pH-adjusted PBS buffer, respectively (the number after N and C represents the corresponding pH values): M, DNA marker for oligonucleotide size evaluation; dT_{30}, GO, and dT_{30}-GO, DI water dissolved dT_{30} oligonucleotides, graphene oxide, and dT_{30}-GO nanocomposite unbuffered suspensions). The black bands in the gel represent the released oligonucleotides from GO nanocomposites. To confirm that the gel bands obtained were from poly dT_{30}, we conducted a control experiment (Supporting Information Figure S5), and our result showed that the poly dT_{30} oligonucleotides were present at two locations in the gels, representing two possible DNA conformations. Both types could be observed in the analysis.

from 1/1 GO and 1/3 GO in the noncompetition groups; by contrast, the dT_{30}-1/5 GO nanocomposite was stable in the noncompetition groups and the oligonucleotides were released only upon protonation of rhodamine in an acidic environment (C4, C5, and C6). Thus, we used 1/5 GO in the subsequent oligonucleotide-bearing nanocarrier studies.

Based on the aforementioned observations, we hypothesized that GOs oxidized to distinct degrees could exert dissimilar effects in the competitive reaction because of the interactions between poly dT_{30} and GO, as well as because of the competition by protonated rhodamine. The interactions between poly dT_{30} and GO could be $\pi-\pi$ stacking hydrophobic interactions and also hydrogen bonding.[30−32] With an increase in the degree of GO oxidation, the number of oxygenated groups generated was increased, which strengthened the hydrogen bonding between poly dT_{30} and GO and caused tight adsorption of poly dT_{30} on the surface of GO. This is probably why, under the conditions N4, N5, N6, and N7, no bands were detected in the case of the dT_{30}-1/5 GO sample. In acidic environments, protonated rhodamine[33] might readily approach proximate dT_{30}-GO through electrostatic attraction, and the $\pi-\pi$ interaction and hydrogen bonding between either rhodamine and GO or rhodamine and dT_{30} might interfere with the adsorption of dT_{30} on GO and thereby strip off the dT_{30} oligonucleotides.

In the following experiments, we added the constructed GO-based nanocomposite to cultured cells and evaluated the performance of the nanoplatforms in simultaneous pH sensing by the fluorescence probe and targeted oligonucleotide delivery. To ensure the cellular uptake of the pH-sensitive rhodamine probe by raw 264.7 cells, we first incubated the cells with 100 μM rhodamine for 0.5, 1, and 2 h and determined that only 0.5 h was required for the probe to enter these cells (Supporting Information Figure S6). Similar procedures were also used to monitor the cellular uptake of GO. The cells were dyed using 100 μM rhodamine for 0.5 h, washed with PBS, and then fed with 100 μg/mL of 1/5 GO for 0.5, 1, and 2 h; subsequently, we monitored the changes in rhodamine fluorescence in the cells by using flow cytometry and confocal microscopy. Flow cytometric analysis revealed that rhodamine fluorescence was quenched within 0.5 h (Figure 6a), which indicated that only a short incubation period is required for the cellular uptake of GOs. We confirmed that the fluorescence intensity was not decreased because of the washing steps. Cells incubated with the medium after the rhodamine probes were removed, and as shown in Figure 6b−d, in the presence of GO, rhodamine fluorescence decreased to a greater extent than it did in the absence of GO. The results revealed that GO can enter cells and that rhodamine fluorescence was quenched upon GO treatment as a result of facilitated adsorption of protonated rhodamine on the GO surface.

To enable the intracellular monitoring of oligonucleotide delivery, we used fluorescent FAM-labeled poly dT_{30} in the next set of experiments. Previous work has demonstrated that GO can quench the fluorescent dye through FRET.[34] We first optimized the concentration ratio of FAM-dT_{30} to GO by measuring the fluorescence of FAM. Approximately 100 μg/mL GO could completely quench the fluorescence of 50 μg/mL FAM-labeled poly dT_{30} (Figure 7), and thus 1/2 was identified as the optimized concentration ratio of FAM-dT_{30} to GO. In the following study, we used this FAM-dT_{30}-GO nanocomposite for oligonucleotide delivery and again monitored the reactions in cells by using flow cytometry (Figure 8) and confocal microscopy (Figure 9).

The rhodamine-triggered competition reaction occurred when the dT_{30}-GO nanocarrier was introduced. As expected, this led to the quenching of rhodamine fluorescence by GO (Figure 6 and Supporting Information Figure S7) and FAM fluorescence recovery as a result of the FAM-dT_{30} oligonucleotide release. As shown in the flow cytometric analysis (Figure 8a,b), the facilitated release of oligonucleotides from the GO nanocarrier could be observed: in the presence of rhodamine, FAM fluorescence recovered to a greater extent than it did in the absence of rhodamine. In addition, we found that this reaction was rapid: only 0.5 h was required for the release of FAM-dT_{30} from GO (Figure 8a,d−f), with an apparent shift to the right in the FAM fluorescence intensity. Our studies also demonstrated that GO facilitated the cellular uptake of oligonucleotides to a greater extent than that observed under the condition in which only FAM-dT_{30} was used (Figure 8c). This finding consistent with previous study[35] indicated that GO could serve as an efficient transfection reagent when developing future gene nanocarriers. Confocal imaging also confirmed the successful delivery of FAM-dT_{30}-GO inside cells (Figure 9). The protonated rhodamine emitted red fluorescence under acid microenvironment. Competitive binding of the rhodamine molecules on GO occurred in cells fed with FAM-dT_{30}-GO, consequently promoting the release of the FAM-dT_{30} oligonucleotides. As a result, the quenching of rhodamine fluorescence and the turning-on of FAM fluorescence could be observed. The concurrent pH sensing and pH-responsive oligonucleotide delivery thus achieved.

The mechanism proposed in most pH-responsive systems employed the idea that the drug release was induced by protonation, resulting in weakened interaction with GO. The

DOI: 10.1021/acsami.5b02397
ACS Appl. Mater. Interfaces 2015, 7, 11467−11475

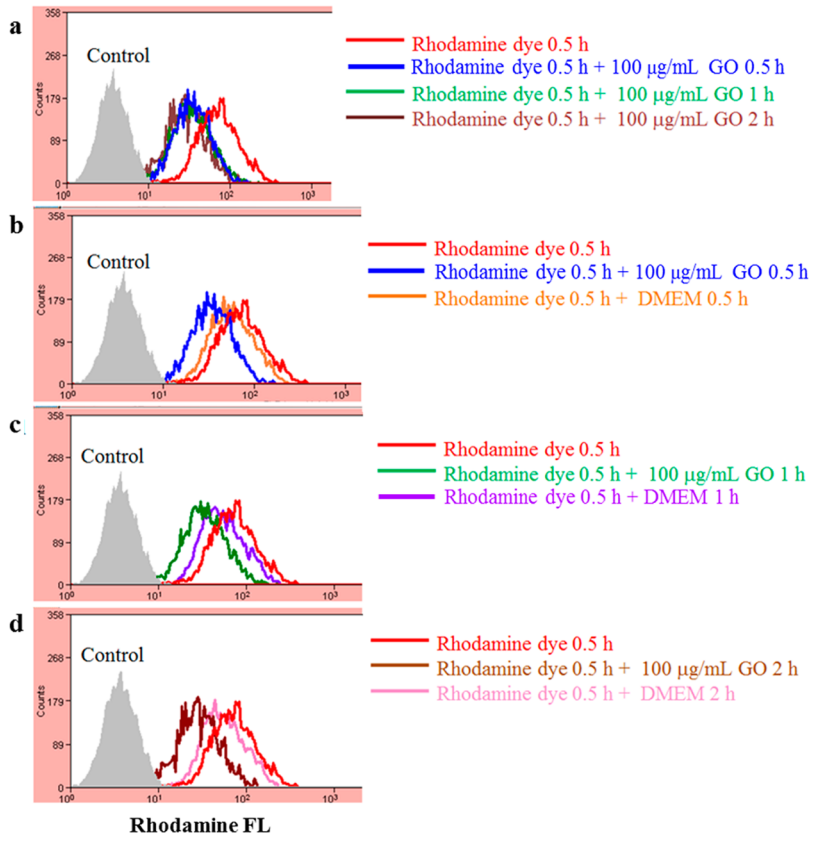

Figure 6. Flow cytometric analysis of GO uptake by raw 264.7 cells. The cells were dyed using 100 μM rhodamine for 0.5 h, washed with PBS, and (a) the rhodamine fluorescence (FL) was monitored in raw 264.7 cells during a 2 h period with or without GO treatment. The quenched FL in raw 264.7 cells was identified after 30 min of incubation (with an apparent shift to the left in the fluorescence intensity). (b–d) Control experiments (using DMEM only cell medium at each incubation time point to wash the cells) were included to confirm only limited FL decrease was observed due to washing steps.

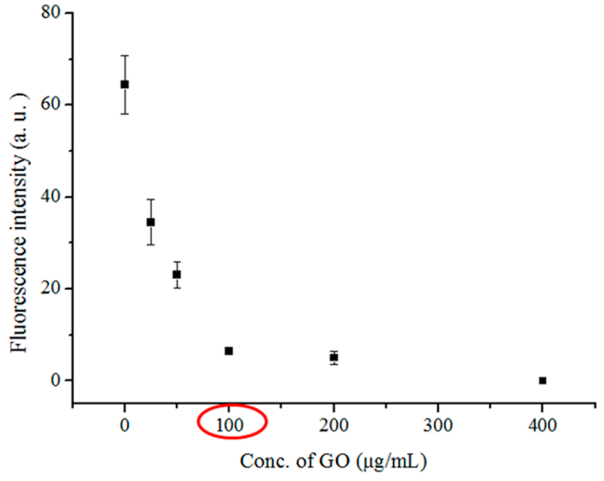

Figure 7. FAM-dT_{30}-GO adsorption kinetics. Complete quenching of the FAM-labeled poly dT_{30} (50 μg/mL) fluorescence was achieved in the presence of 100 μg/mL graphene oxide (GO).

oxidation status of GO was not tuned in these cases[3,5,17,19] (usually 1/3 mass ratio of graphite and $KMnO_4$ was applied according to the original Hummers' method). But nevertheless, due to the fact that various modifications in reaction time, temperature, and multiple oxidizing agents were adopted during the GO preparation, it was difficult to examine and compare the exact oxidation status among these GO-based nanocarriers. Based on our findings, however, highly oxidized GO actually forms stable complex with oligonucleotides under acidic conditions, the delivery efficiency thus can be altered or ineffective, depending on the oxidation extent of prepared GO when considering the mechanism mentioned earlier. We demonstrated an alternative competition-facilitated intracellular drug delivery system in which the oligonucleotide release was finely controlled, initiating via the protonation of rhodamine tracer upon acidic pH stimuli followed by its competition reaction at the GO surface. Nonetheless, we also observed a small amount of non-pH-specific leakage of FAM-dT_{30} in the cells during the time in the absence of rhodamine pretreatment (Figure 9 and Supporting Information Figure S8). This nonspecific desorption might be caused by the presence of biomolecules in the complex cell culture medium: Biomolecules such as proteins, antigens, antibodies, and hormones have been reported to interact with GO and release nucleotides from the surface of GO.[36,37] This may be an issue that we shall overcome to improve the GO-based nanocarrier stabilization in future work.

CONCLUSION

In summary, we investigated a series of GOs oxidized to distinct degrees and determined that the most highly oxidized GO was able to stabilize the immobilized oligonucleotides at its surface even under acidic conditions. We propose a critical role of GO oxidation status in designing the gene nanocarrier. Simplified preparation was achieved by comparing with conventional methods in which functionalization of polymers

DOI: 10.1021/acsami.5b02397
ACS Appl. Mater. Interfaces 2015, 7, 11467–11475

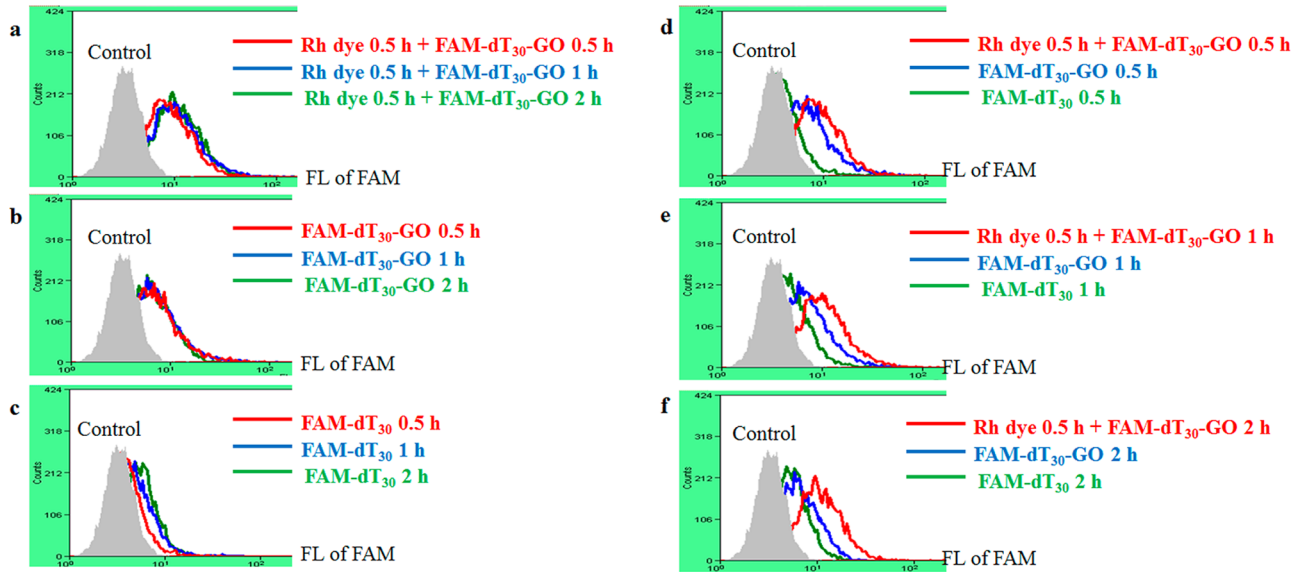

Figure 8. Flow cytometric analysis of rhodamine-triggered competition reaction after introducing the FAM-dT_{30}-GO nanocomposite. The cells were dyed by using 100 μM rhodamine for 0.5 h and being washed with PBS, and the FAM fluorescence (FL) was monitored in raw 264.7 cells during a 2 h period in the (a) presence or (b) absence of rhodamine, and an additional control experiment was performed using (c) FAM-labeled oligonucleotides dT_{30} only. (d–f) The recovery of FAM fluorescence in rhodamine-triggered competition reaction could be observed with an apparent shift to the right in the fluorescence intensity during the time ([1/5 GO], 50 μg/mL; [FAM-dT_{30}], 25 μg/mL; [rhodamine], 100 μM).

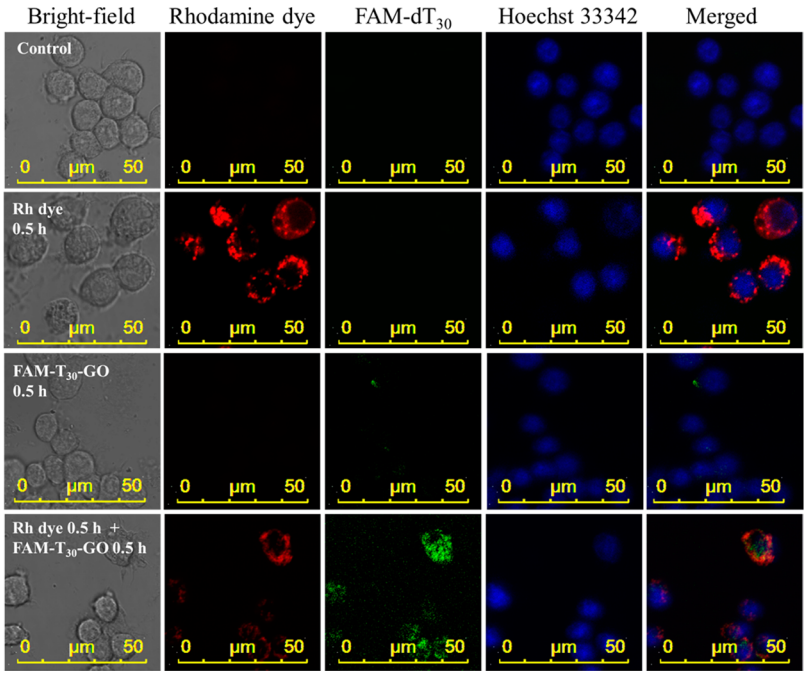

Figure 9. Competition-facilitated intracellular drug delivery monitored using confocal microscopy. The protonated rhodamine emitted red fluorescence (λ_{ex} = 561 nm, λ_{em} = 588 nm) under acid microenvironment. Cells fed with FAM-dT_{30}-GO led to the competitive binding of rhodamine on GO and consequently the quenching of its fluorescence and promoted the release of the FAM-dT_{30} oligonucleotides. As a result, the turning-on of FAM fluorescence (λ_{ex} = 488 nm, λ_{em} = 517 nm) could be observed (Hoechst 33342, blue, for nucleus staining; merged, overlay of all fluorescence images).

was usually required at the interface of GO and oligonucleotides to stabilize the complex.[17,19,38,39] Such types of GO also performed most favorably in the rhodamine-poly dT_{30} oligonucleotide competition reaction. We labeled poly dT_{30} with FAM fluorescent dye in order to monitor the intracellular release of oligonucleotides, and using flow cytometry and confocal microscopy we confirmed pH-responsive, competition-facilitated drug release in this setup, which enables high drug loading (FAM-dT_{30}/GO = 25/50 μg/mL) and rapid cellular uptake (<0.5 h). This study provides a new drug-delivery strategy which can precisely monitor the acidic microenvironment and control the consequent oligonucleotides release upon drug nanocarrier treatment by simple observation of the turn on/off of rhodamine fluorescence. Our approach offers insights for future pH-triggered tumor targeting for the delivery of new generation RNAi drugs.

DOI: 10.1021/acsami.5b02397
ACS Appl. Mater. Interfaces 2015, 7, 11467–11475

■ ASSOCIATED CONTENT

Supporting Information

Images of pH-sensitive rhodamine, additional GO characterization data, agarose gel electrophoresis of control samples, cellular uptake of rhodamine, further flow cytometric analysis, and confocal images. The Supporting Information is available free of charge on the ACS Publications website at DOI: 10.1021/acsami.5b02397.

■ AUTHOR INFORMATION

Corresponding Author

*Tel.: +886-(0)3-5712121 ext. 56556. Fax: +886-(0)3-5723764. E-mail: hyhsu99@nctu.edu.tw.

Notes

The authors declare no competing financial interest.

■ ACKNOWLEDGMENTS

This work has been supported by the Ministry of Science and Technology of Taiwan (Grant No. MOST103-2113-M-009-006) and the Ministry of Education, Taiwan (Aim for the Top University Plan (MOE-ATU) program of National Chiao-Tung University).

■ REFERENCES

(1) Yang, Z.; Wang, H.; Zhao, J.; Peng, Y.; Wang, J.; Guinn, B.; Huang, L. Recent Developments in the Use of Adenoviruses and Immunotoxins in Cancer Gene Therapy. *Cancer Gene Ther.* **2007**, *14*, 599−615.

(2) Naldini, L.; Blömer, U.; Gallay, P.; Ory, D.; Mulligan, R.; Gage, F. H.; Verma, I. M.; Trono, D. In Vivo Gene Delivery and Stable Transduction of Nondividing Cells by a Lentiviral Vector. *Science* **1996**, *272*, 263−267.

(3) Zhang, L.; Xia, J.; Zhao, Q.; Liu, L.; Zhang, Z. Functional Graphene Oxide as a Nanocarrier for Controlled Loading and Targeted Delivery of Mixed Anticancer Drugs. *Small* **2010**, *6*, 537−544.

(4) Choi, D.; Jeong, H.; Kim, K. Electrochemical Thrombin Detection Based on the Direct Interaction of Target Proteins and Graphene Oxide as an Indicator. *Analyst* **2014**, *139*, 1331−1333.

(5) Sun, X.; Liu, Z.; Welsher, K.; Robinson, J.; Goodwin, A.; Zaric, S.; Dai, H. Nanographene Oxide for Cellular Imaging and Drug Delivery. *Nano Res.* **2008**, *1*, 203−212.

(6) Lin, D.; Wu, J.; Wang, M.; Yan, F.; Ju, H. Triple Signal Amplification of Graphene Film, Polybead Carried Gold Nanoparticles as Tracing Tag and Silver Deposition for Ultrasensitive Electrochemical Immunosensing. *Anal. Chem.* **2012**, *84*, 3662−3668.

(7) Lu, C.-H.; Zhu, C.-L.; Li, J.; Liu, J.-J.; Chen, X.; Yang, H.-H. Using Graphene to Protect DNA from Cleavage During Cellular Delivery. *Chem. Commun. (Cambridge, U. K.)* **2010**, *46*, 3116−3118.

(8) Tang, Z.; Wu, H.; Cort, J. R.; Buchko, G. W.; Zhang, Y.; Shao, Y.; Aksay, I. A.; Liu, J.; Lin, Y. Constraint of DNA on Functionalized Graphene Improves Its Biostability and Specificity. *Small* **2010**, *6*, 1205−1209.

(9) Feng, L.; Zhang, S.; Liu, Z. Graphene Based Gene Transfection. *Nanoscale* **2011**, *3*, 1252−1257.

(10) Chen, B.; Liu, M.; Zhang, L.; Huang, J.; Yao, J.; Zhang, Z. Polyethylenimine-Functionalized Graphene Oxide as an Efficient Gene Delivery Vector. *J. Mater. Chem.* **2011**, *21*, 7736−7741.

(11) Kim, H.; Kim, W. J. Photothermally Controlled Gene Delivery by Reduced Graphene Oxide−Polyethylenimine Nanocomposite. *Small* **2014**, *10*, 117−126.

(12) Stubbs, M.; McSheehy, P. M. J.; Griffiths, J. R.; Bashford, C. L. Causes and Consequences of Tumour Acidity and Implications for Treatment. *Mol. Med. Today* **2000**, *6*, 15−19.

(13) Yu, J.; Chu, X.; Hou, Y. Stimuli-Responsive Cancer Therapy Based on Nanoparticles. *Chem. Commun. (Cambridge, U. K.)* **2014**, *50*, 11614−11630.

(14) Goenka, S.; Sant, V.; Sant, S. Graphene-Based Nanomaterials for Drug Delivery and Tissue Engineering. *J. Controlled Release* **2014**, *173*, 75−88.

(15) He, X.; Li, J.; An, S.; Jiang, C. pH-Sensitive Drug-Delivery Systems for Tumor Targeting. *Ther. Delivery* **2013**, *4*, 1499−1510.

(16) Yang, X.; Wang, Y.; Huang, X.; Ma, Y.; Huang, Y.; Yang, R.; Duan, H.; Chen, Y. Multi-Functionalized Graphene Oxide Based Anticancer Drug-Carrier with Dual-Targeting Function and pH-Sensitivity. *J. Mater. Chem.* **2011**, *21*, 3448−3454.

(17) Kavitha, T.; Haider Abdi, S. I.; Park, S.-Y. pH-Sensitive Nanocargo Based on Smart Polymer Functionalized Graphene Oxide for Site-Specific Drug Delivery. *Phys. Chem. Chem. Phys.* **2013**, *15*, 5176−5185.

(18) Fan, X.; Jiao, G.; Gao, L.; Jin, P.; Li, X. The Preparation and Drug Delivery of a Graphene-Carbon Nanotube-Fe_3O_4 Nanoparticle Hybrid. *J. Mater. Chem. B* **2013**, *1*, 2658−2664.

(19) Rana, V. K.; Choi, M. C.; Kong, J. Y.; Kim, G. Y.; Kim, M. J.; Kim, S. H.; Mishra, S.; Singh, R. P.; Ha, C. S. Synthesis and Drug-Delivery Behavior of Chitosan-Functionalized Graphene Oxide Hybrid Nanosheets. *Macromol. Mater. Eng.* **2011**, *296*, 131−140.

(20) Tao, C.-a.; Wang, J.; Qin, S.; Lv, Y.; Long, Y.; Zhu, H.; Jiang, Z. Fabrication of pH-Sensitive Graphene Oxide−Drug Supramolecular Hydrogels as Controlled Release Systems. *J. Mater. Chem.* **2012**, *22*, 24856−24861.

(21) Zhu, L.; Luo, L.; Wang, Z. DNA Electrochemical Biosensor Based on Thionine-Graphene Nanocomposite. *Biosens. Bioelectron.* **2012**, *35*, 507−511.

(22) Wang, X.-Y.; Gao, A.; Lu, C.-C.; He, X.-W.; Yin, X.-B. An Electrochemiluminescence Aptasensor for Thrombin Using Graphene Oxide to Immobilize the Aptamer and the Intercalated Probe. *Biosens. Bioelectron.* **2013**, *48*, 120−125.

(23) Song, Y.; Qu, K.; Zhao, C.; Ren, J.; Qu, X. Graphene Oxide: Intrinsic Peroxidase Catalytic Activity and Its Application to Glucose Detection. *Adv. Mater.* **2010**, *22*, 2206−2210.

(24) Chang, H.; Tang, L.; Wang, Y.; Jiang, J.; Li, J. Graphene Fluorescence Resonance Energy Transfer Aptasensor for the Thrombin Detection. *Anal. Chem.* **2010**, *82*, 2341−2346.

(25) Song, J.; Lau, P. S.; Liu, M.; Shuang, S.; Dong, C.; Li, Y. A General Strategy to Create RNA Aptamer Sensors Using "Regulated" Graphene Oxide Adsorption. *ACS Appl. Mater. Interfaces* **2014**, *6*, 21806−21812.

(26) Viraka Nellore, B. P.; Kanchanapally, R.; Pramanik, A.; Sinha, S. S.; Chavva, S. R.; Hamme, A.; Ray, P. C. Aptamer-Conjugated Graphene Oxide Membranes for Highly Efficient Capture and Accurate Identification of Multiple Types of Circulating Tumor Cells. *Bioconjugate Chem.* **2015**, *26*, 235−242.

(27) Chen, R. J.; Zhang, Y. Controlled Precipitation of Solubilized Carbon Nanotubes by Delamination of DNA. *J. Phys. Chem. B* **2006**, *110*, 54−57.

(28) Liu, S.-R.; Wu, S.-P. New Water-Soluble Highly Selective Fluorescent Chemosensor for Fe(III) Ions and Its Application to Living Cell Imaging. *Sens. Actuators, B* **2012**, *171*−*172*, 1110−1116.

(29) Hummers, W. S., Jr.; Offeman, R. E. Preparation of Graphitic Oxide. *J. Am. Chem. Soc.* **1958**, *80*, 1339−1339.

(30) Premkumar, T.; Geckeler, K. E. Graphene−DNA Hybrid Materials: Assembly, Applications, and Prospects. *Prog. Polym. Sci.* **2012**, *37*, 515−529.

(31) Park, J. S.; Na, H.-K.; Min, D.-H.; Kim, D.-E. Desorption of Single-Stranded Nucleic Acids from Graphene Oxide by Disruption of Hydrogen Bonding. *Analyst* **2013**, *138*, 1745−1749.

(32) Wu, M.; Kempaiah, R.; Huang, P.-J. J.; Maheshwari, V.; Liu, J. Adsorption and Desorption of DNA on Graphene Oxide Studied by Fluorescently Labeled Oligonucleotides. *Langmuir* **2011**, *27*, 2731−2738.

DOI: 10.1021/acsami.5b02397
ACS Appl. Mater. Interfaces 2015, 7, 11467−11475

(33) Chen, X.; Pradhan, T.; Wang, F.; Kim, J. S.; Yoon, J. Fluorescent Chemosensors Based on Spiroring-Opening of Xanthenes and Related Derivatives. *Chem. Rev.* **2011**, *112*, 1910−1956.
(34) Li, S.; Aphale, A. N.; Macwan, I. G.; Patra, P. K.; Gonzalez, W. G.; Miksovska, J.; Leblanc, R. M. Graphene Oxide as a Quencher for Fluorescent Assay of Amino Acids, Peptides, and Proteins. *ACS Appl. Mater. Interfaces* **2012**, *4*, 7069−75.
(35) Wang, Y.; Li, Z.; Hu, D.; Lin, C.-T.; Li, J.; Lin, Y. Aptamer/Graphene Oxide Nanocomplex for in Situ Molecular Probing in Living Cells. *J. Am. Chem. Soc.* **2010**, *132*, 9274−9276.
(36) Hong, B. J.; An, Z.; Compton, O. C.; Nguyen, S. T. Tunable Biomolecular Interaction and Fluorescence Quenching Ability of Graphene Oxide: Application to ″Turn-on″ DNA Sensing in Biological Media. *Small* **2012**, *8*, 2469−2476.
(37) Tan, X.; Chen, T.; Xiong, X.; Mao, Y.; Zhu, G.; Yasun, E.; Li, C.; Zhu, Z.; Tan, W. Semiquantification of ATP in Live Cells Using Nonspecific Desorption of DNA from Graphene Oxide as the Internal Reference. *Anal. Chem.* **2012**, *84*, 8622−8627.
(38) Liu, Z.; Robinson, J. T.; Sun, X.; Dai, H. PEGylated Nanographene Oxide for Delivery of Water-Insoluble Cancer Drugs. *J. Am. Chem. Soc.* **2008**, *130*, 10876−10877.
(39) Chen, T.-T.; Tian, X.; Liu, C.-L.; Ge, J.; Chu, X.; Li, Y. Fluorescence Activation Imaging of Cytochrome c Released from Mitochondria Using Aptameric Nanosensor. *J. Am. Chem. Soc.* **2015**, *137*, 982−989.

DOI: 10.1021/acsami.5b02397
ACS Appl. Mater. Interfaces 2015, 7, 11467−11475